Peer-reviewed version available at Biomolecules 2018, 8, 161; doi:10.3390/biom8040161

Review

Structural and Functional Insights into Human Nuclear Cyclophilins

Caroline Rajiv[12] and Tara L. Davis[13,*]

[1] Department of Biochemistry and Molecular Biology, Drexel University College of Medicine, Philadelphia PA USA 19102.
[2] Janssen Pharmaceuticals, Inc., 22-21062, 1400 McKean Rd, Spring House, PA 19477; caroline.rajiv@gmail.com
[3] FORMA Therapeutics, 550 Arsenal St. Ste. 100, Boston, MA 02472; tdavis@formatherapeutics.com

* Correspondence: tdavis@formatherapeutics.com; Tel.: +01-857-209-2342

Abstract: The peptidyl-prolyl isomerases of the cyclophilin type are distributed throughout human cells, including eight found solely in the nucleus. Nuclear cyclophilins are involved in complexes that regulate chromatin modification, transcription, and pre-mRNA splicing. This review collects what is known about the eight human nuclear cyclophilins: PPIH, PPIE, PPIL1, PPIL2, PPIL3, PPIG, CWC27, and PPWD1. Each "spliceophilin" is evaluated in relation to the spliceosomal complex in which it has been studied, and current work studying the biological roles of these cyclophilins in the nucleus are discussed. The eight human splicing complexes available in the RCSB are analyzed from the viewpoint of the human spliceophilins. Future directions in structural and cellular biology, and the importance of developing spliceophilin-specific inhibitors, are considered.

Keywords: Peptidyl-prolyl isomerases; nuclear cyclophilins; spliceophilins; alternative splicing; spliceosomes; NMR; x-ray crystallography

1. Introduction

Cyclophilins are members of the peptidyl prolyl isomerase (PPI) family, along with the structurally unrelated FK506 binding proteins and the parvulins (EC 5.2.1) [1-3]. Cyclophilins are evolutionally widespread, with paralog cyclophilins found in all kingdoms of life, including viruses. In many species there exist multiple cyclophilins encoded in the genome; depending on how strictly one defines a sequence as cyclophilin-like, there are anywhere from 17-30 cyclophilins encoded in humans [1,2,4]. In humans, as in other multicellular organisms, when multiple cyclophilin family members are encoded, they are also often found targeted to multiple cellular compartments. This is the case in humans, where cyclophilins are distributed throughout the cell. One family member, PPIF, is targeted to mitochondria, where it participates in regulation of the mitochondrial permeability transition pore [5-7]. The three cytoplasmic cyclophilins – the canonical family member PPIA, plus PPIB and PPIC – have also been detected extracellularly in various reports. Most biological studies have focused on the mechanisms by which these three cyclophilins facilitate host:viral interactions, particularly for HIV and hepatitis A, B, and C [8-10]. Much less is known about the cytoplasmic cyclophilins PPID, PPIL4, RANBP2, and the nuclear cyclophilins PPIL6 and NKTR, and these will not be discussed further here. The purpose of this review is to highlight what is currently known about the structure and biological function of the eight human nuclear-localized cyclophilins: PPIE, PPIG, PPIH, PPIL1, PPIL2, PPIL3, PPWD1, and CWC27.

Cyclophilin domains are characterized by a central closed-barrel type beta fold, with large regions of ordered loops and two small helices packed against the loop region and sheets β7- β8 of the central barrel (SCOP fold family 50892). See Figure 1 for the structure of the canonical family member PPIA.

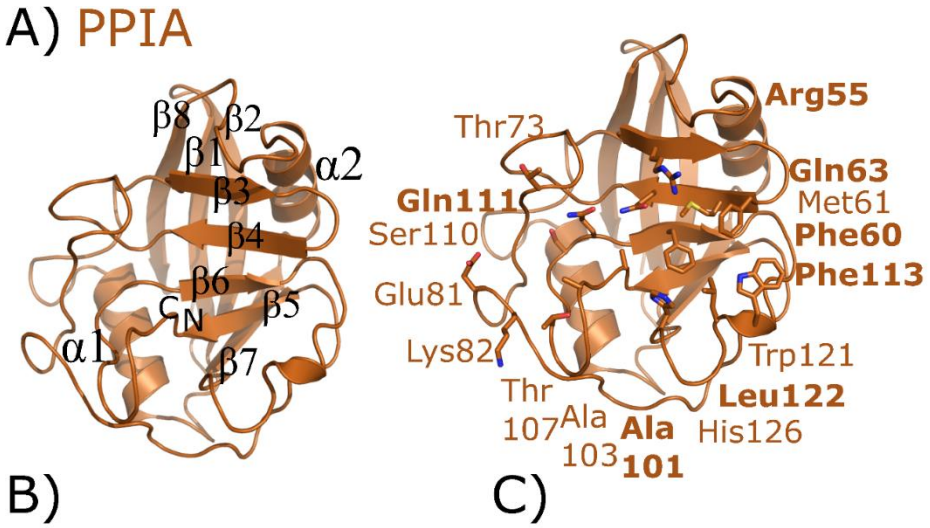

B)

PPIA residue	55	60	61	63	101	113	121	122	126
PPIA	Arg	Phe	Met	Gln	Ala	Phe	Trp	Leu	His
PPIE	Arg	Phe	Met	Gln	Ala	Phe	Trp	Leu	His
PPIG	Arg	Phe	Met	Gln	Ala	Phe	His	Leu	His
PPIH	Arg	Phe	Met	Gln	Ala	Phe	Trp	Leu	His
PPIL1	Arg	Phe	Met	Gln	Ala	Phe	Trp	Leu	His
PPIL2	Arg	Phe	Val	Gln	Ala	Phe	Tyr	Leu	His
PPIL3	Arg	Phe	Met	Gln	Ala	Phe	His	Leu	Tyr
PPWD1	Arg	Phe	Met	Gln	Ala	Phe	Trp	Leu	His
CWC27	Arg	Phe	Ile	Gln	Ala	Phe	Glu	Leu	His

C)

PPIA residue	73	81	82	103	107	110	111
PPIA	thr	glu	lys	ala	thr	ser	gln
PPIE	thr	lys	lys	ser	thr	ser	gln
PPIG	arg	gly	phe	arg	thr	ser	gln
PPIH	thr	gly	pro	ser	thr	cys	gln
PPIL1	thr	lys	gln	ala	thr	ser	gln
PPIL2	thr	lys	pro	ser	ser	ser	gln
PPIL3	arg	lys	lys	asn	thr	ser	gln
PPWD1	met	gly	glu	ala	thr	ser	gln
CWC27	ser	ala	pro	ala	asp	ser	gln

Figure 1. Structure and annotation of the canonical cyclophilin peptidyl-prolyl isomerase A (PPIA). Left panel, secondary structural elements are labeled for the PDB 2CPL. Right panel, residues that comprise the S1 (proline-binding) and S2 (specificity) pockets are shown in stick representation and labeled. S1 pocket labels are on the right, S2 pocket labels on the left, and in bold are residues absolutely invariant across the nuclear cyclophilin family relative to PPIA. Residue numbering also follows PPIA, by convention. (B) The residues that comprise the S1 pockets are largely invariant, while (C) the residues that comprise the S2 pockets are more variable.

Additionally, many cyclophilin family members in more complex organisms encode for additional motifs and domains (see Figure 2), discussed in further detail below for the human nuclear cyclophilins PPIE, PPIG, PPIL2, PPWD1, and CWC27. Originally characterized as the protein receptor for the natural product cyclosporine, cyclophilins have long been studied *in vitro* because of their high solubility and attractive biophysical properties. Decades of structural work utilizing well-behaved cyclophilins have led to nearly complete coverage of the human cyclophilin family, by both x-ray crystallography and NMR [2,11-15]. These structures have been used to facilitate studies focused on substrate specificity and selective pharmacophores, persistent issues in the field due to the high degree of sequence identity within the S1 pocket (Figure 1B). It is likely that specificity in this family, if focused on the active site, will depend on rational design focusing on the less conserved S2 pocket, contiguous to S1 (Figure 1A, 1C) [10,16]. An opinion of the utility of design against the S2 pocket for the nuclear cyclophilins will be addressed at the end of this review. It is structural information for complexes containing the nuclear cyclophilins, rather than structures of the cyclophilins alone, that have been most informative in studying the regulation of transcription and of pre-mRNA splicing [2,15-22]. There are multiple cryo-EM structures of spliceosomal complexes that contain one or more of the nuclear cyclophilins; with some technical caveats, these structures can also add crucial information to the ways in which this sub-set of the cyclophilin family may regulate nuclear processes [23-28]. It seems clear that cyclophilins participate uniquely in nuclear function,

Preprints (www.preprints.org) | NOT PEER-REVIEWED | Posted: 2 November 2018 doi:10.20944/preprints201811.0037.v1

Peer-reviewed version available at Biomolecules 2018, 8, 161; doi:10.3390/biom8040161

despite their apparent structural similarity. We will present each cyclophilin individually to allow us to highlight their unique nature.

2. Background and Structures of the Nuclear Cyclophilins

The domain organization of the nuclear cyclophilins, along with the canonical family member PPIA, and their association with splicing complexes and sub-complexes, is depicted in Figure 2.

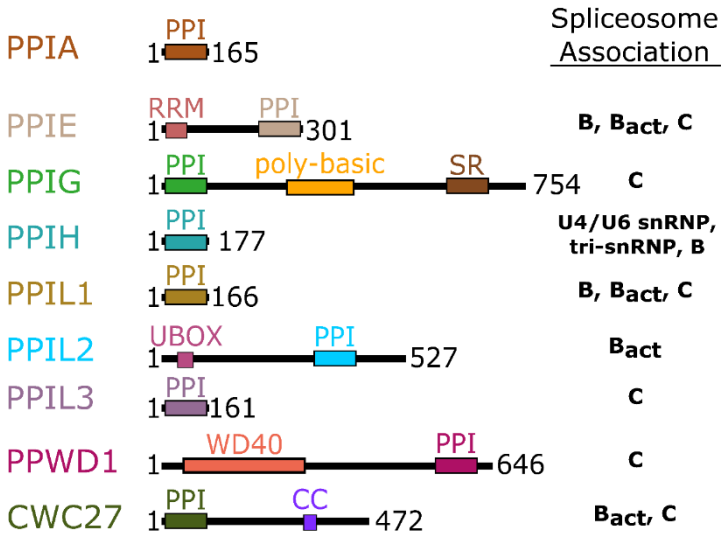

Figure 2. Figure 2. Domain organization of the nuclear cyclophilins. Colors are consistent throughout all figures. Spliceosome association is modified from [34,35].

Bioinformatics from several sources are collated in Table 1 for the nuclear cyclophilins. Additional information, including full amino acid sequences, can be found in Supplemental Table 1.

Table 1. Selected bioinformatics for the nuclear cyclophilins.

Gene Name	UniProt Accession	# aa	Domain 1	Boundary	Domain 2	Boundary	Cryo-EM structures
PPIA	P62937	165	PPI	1-165			
PPIE	Q9UNP9	301	RRM	7-80	PPI	143-299	5MQF, 5YZG, 5Z56, 5Z57
PPIG	Q13427	754	PPI	11-176	SR/RS repeats	540-639	5YZG
PPIH	O43447	177	PPI	1-177			5O9Z
PPIL1	Q9Y3C6	166	PPI	1-166			5MQF, 5XJC, 5YZG, 5Z56, 5Z57, 6FF4
PPIL2	Q13356	527	UBOX	42-101	PPI	281-433	
PPIL3	Q9H2H8	161	PPI	1-161			
PPWD1	Q96BP3	646	WD40	80-453	PPI	490-645	5YZG
CWC27	Q6UX04	472	PPI	14-166	coiled-coil	306-351	5Z56, 5Z58, 6FF4

2.1. PPIH

Peptidyl-prolyl isomerase isoform H (PPIH) is a minimal cyclophilin, meaning that it encodes for a single cyclophilin domain. In early publications, Cyp-H, USA-Cyp, or U4/U6-20K were used to designate PPIH [29,30]. The *apo* structure of PPIH was initially published in 2000 and was then solved in complex with a 30-mer peptide derived from its spliceosomal binding partner, pre-mRNA processing factor 4 (PRPF4; not to be confused with PRP4, a nuclear kinase) (Figure 3) [31-33]. PPIH can be considered the first cyclophilin that associates with the spliceosome; it is present within the stand-alone tri-snRNP complex, and integrates into the splicing machinery as part of the transition into the early intermediate B complex [34,35]. PPIH is short-lived within splicing complexes and is not detectable within the spliceosome during later pre-catalytic B_{act} or B* stages [35]. A structure of complex B containing the first visualization of PPIH in a splicing complex, albeit with the aid of cross-linking reagents, has been recently published [28].

The initial interaction between PPIH and PRPF4 was identified as a result of yeast two-hybrid studies [29,30,31]. It was notable at the time that this interaction occurred distal to the active site of PPIH, did not involve interaction with a target proline in PRPF4, and was unaffected by cyclosporine (Figure 3A). More recently, our group has delved more deeply into the relationship between PPIH and PRPF4 and have discovered that there is a second site of interaction that does involve the active site of PPIH and the N-terminus of PRPF4 [17]. However, rather than being crucial for a conformational change within PRPF4, we propose a model in which this interaction instead is mutually beneficial in protecting PRPF4 from un-regulated PTMs in its intrinsically disordered N-terminal region, while also blocking the active site of PPIH from un-regulated proline binding and turnover (Figure 3B). This may well be a general phenomenon within the spliceosome-associated cyclophilins - or, as we call them, the "spliceophilins" - considering the observation of other cyclophilin-centric interactions within the spliceosome that clearly do not involve proline binding outlined later within this review. Unfortunately for those interested in PPIH interactions within the spliceosome, both purified tri-snRNP and B complexes from *Schizomyces pombe* and from human tissue culture lines have been shown to contain PPIH in solution, but fail to visualize the protein in the resulting structures. However, a recent structure of the pre-catalytic B complex captured PPIH via crosslinking, and the authors were able to model the interaction between the critical phenylalanine residue from PRPF4 and the α1-β3 loop of PPIH, thereby recapitulating what had previously been seen in the binary structure (Figure 3C) [28]. The N-terminal region of PRPF4 was not modeled, and so the second site characterized in Rajiv *et. al.* could not be confirmed. However, PPIH is near three additional spliceosomal proteins not yet studied for PPIH interaction *in vitro*: WBP4, PRPF6, and PRPF8. These interactions might prove critical to understanding the function of PPIH in regulation of splicing, and we await further characterization of these interactions with purified proteins *in vitro*.

Preprints (www.preprints.org) | NOT PEER-REVIEWED | Posted: 2 November 2018 doi:10.20944/preprints201811.0037.v1

Peer-reviewed version available at Biomolecules 2018, 8, 161; doi:10.3390/biom8040161

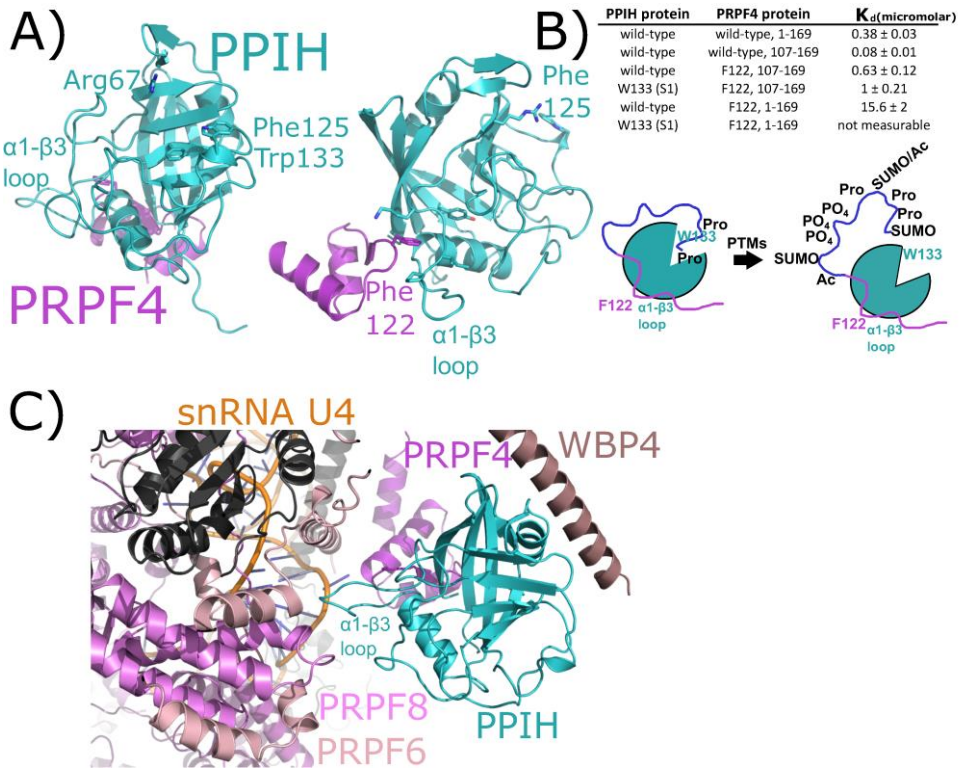

Figure 3. The interaction between PPIH and PRPF4 seen in solution is preserved in early spliceosomes. (A) The complex between a small peptide from PRPF4 and the PPIH protein is shown in cartoon representation (PDB 2MZW) [31]. Key catalytic site residues are highlighted, and in the right panel the high-affinity interaction between Phe122 and the α1-β3 loop of PPI is shown. In (B), a table summarizing the high- and low- affinity sites between PRPF4 and PPIH. Below, a model of the proposed function of the high- and low- affinity sites. Both modified from [17]. (C) The neighborhood around PPIH in the B complex human spliceosome (PDB 5O9Z). In addition to the previously known interaction with PRPF4, potential interactions with WBP4, PRPF6, and PRPF8 are highlighted. U4 snRNA is within 10Å of PPIH and is labeled. Proteins in dark grey are further than 10Å away from PPIH and are not candidates for direct interaction, so are not labeled. The region of PRPF4 forming the low-affinity interaction with PPIH (the extreme N-terminal 100 residues) is disordered in this structure.

2.2. PPIE

Peptidyl-prolyl isomerase isoform E (PPIE) is a multi-domain cyclophilin, encoding for an N-terminal RNA recognition motif (RRM) and a C-terminal cyclophilin domain (Figure 2). Initial studies called PPIE Cyp33. The structure of the cyclophilin domain of PPIE was first solved and deposited as part of a structural genomics initiative, the SGC (Structural Genomics Consortium) [36], later described in Davis et. al. [2]. A slightly lower-resolution structure was independently deposited and described in a publication by Wang et. al. [37], and a modest resolution structure of the same domain was deposited once again in 2011 by the JCSG (Joint Center for Structural Genomics) [38]. Likewise, a structure of the RRM motif of PPIE was originally solved as part of the RIKEN initiative [39], and five years later independently published by three groups [40-42]. Finally, a chimeric structure of the RRM motif of PPIE fused to the PHD motif of MLL1 has been published (Figure 4B) [40]. All PPIE structures, whether of the PPI domain or of the RRM motif, are largely superimposable (Figure 4A). PPIE is a moonlighting cyclophilin, participating in nuclear processes independent of mRNA splicing. A series of studies in 2010 found that both the RRM and cyclophilin domain of PPIE participated in chromatin remodeling complexes [37,40-42]. Using *in vitro* assays, structural analysis, and cellular assays, the RRM motif was found to interact directly with the PHD3 domain in the histone reader MLL1, while the cyclophilin domain interacts with a proline in MLL1 to allow for the RRM:PHD complex to form. The RRM interaction surface was found to be extensive, including

residues from all four central beta sheets in the RRM (Figure 4B) [40-42]. A separate study identified PPIE as part of the XAB2 complex, a subset of spliceosomal proteins (XAB2 (SYF1), AQR, CCDC16, ISY1, and PPIE) that binds RNA but also participates in transcription-coupled DNA repair in cells [43]. The XAB2 complex was later termed the IBC (intron binding complex), and the RNA interaction was characterized in much greater detail [44,45]. No specific interactions between AQR and PPIE, or other proteins within the IBC, have been validated *in vitro*.

PPIE an early spliceophilin; it is part of the "PRP19 complex" and is first present with low abundance in B complex. As with other PRPF19 complex members, PPIE is highly abundant in the later intermediate complexes B* and B_{act}, and is also abundant in the catalytic C complex [34,35]. Versions of all three of these complexes have been published out of *S. pombe* and human, but PPIE has only been visualized in human complexes [23,24,27].

In human spliceosomes PPIE has been built into four structures: two representing pre-catalytic B complexes, and two representing the catalytic C complex [23,24,27]. Both the RRM and cyclophilin domains are modeled into density in all these structures, providing novel insight into the particular interactions mediated by each domain. In the "mature B_{act}" structure, the region around proline 83 of SF3B4 is pointed towards the active site of PPIE (Figure 4C). Other interactors include SF3B2, also with the catalytic face of PPIE, and SF3A2, which interacts both with the PPI and RRM domain of PPIE. In addition to extensive contact with SF3A2, the RRM motif is also potentially interacting with SYF1. These interactions are largely with the alpha-helix and loop regions of RRM, as opposed to the beta-sheet mediated interaction with MLL1 (Figure 4B). In the "late B_{act}" spliceosome, this protein network surrounding PPIE is largely unchanged.

Finally, the two catalytic complexes that model PPIE do so in very different orientations. In the "step 1" catalytic C complex, the PPI domain of PPIE is interacting with ISY1, SNRNP A', and SNRNP B/B', with SmD3 closely associated with SNRNP A' and B/B'. The RRM interaction with SYF1 is preserved. Visible in this structure is the position of the pre-mRNA substrate, which seems to interact directly with the long β2-β3 loop in the RRM (Figure 4E). Also interacting with the RRM motif is AQR and SNRNP A'. In the C* complex spliceosome published in Bertram *et. al.*, the interaction with SYF1 and AQR is mediated through the PPI domain of PPIE rather than the RRM motif, and the model of U2snRNA is placed extremely close to PPIE. In this structure the orientation of PPIE seems to be flipped, with the PPI domain interacting with AQR and SYF1, and the RRM motif close to PRPF17. Perhaps future structures will resolve this seeming discrepancy.

Figure 4. Structures of PPIE in solution and in spliceosomes. In (A), the cyclophilin and RRM domains of PPIE are shown in cartoon representation. The PPI domain is represented by an overlay of PDB codes 2R99, 1ZMF, and 3UCH. Selected catalytic residues and protein:protein interaction regions are labeled. The RRM domain is represented by an overlay of PDBs 2CQB, 2KU7, 2KYX, 3LPY, and 3MDF (chain A only). Secondary structure elements are labeled. (B) The RRM of PPIE was previously shown to interact with the PHD domain of MLL through an extensive interface involving multiple β-strands. (C) The neighborhood of the PPIE PPI (left) and RRM (right) domains in the "mature Bact" spliceosome is shown (PDB 5Z56). The region around Pro83 of SF3B4 is pointed towards the active site of PPIE (marked with an asterisk). Other interactors are in color and labeled. (D) The neighborhood of the PPIE PPI (bottom center) and RRM (top center) domains in the "late Bact" spliceosome is shown (PDB 5Z57). The protein network surrounding PPIE is unchanged relative to those shown in (C), but in this view SF3A3 is visible, which is just within 10Å of PPIE PPI domain. (E) The neighborhood of the PPIE PPI (left) and RRM (right) domains in the C complex spliceosome (PDB 5YZG). Highlighted on the left panel are interactions between the PPI domain and SNRNP A', B/B', and SmD3 along with ISY1. Visible in this structure is the position of the pre-mRNA substrate, which is interacting with the RRM motif. In the right panel, other RRM interactors including SYF1, AQR, and SNRPA'. The PPI domain is visible in the lower right corner for reference. (F) The neighborhood of the PPIE PPI (left) and RRM (right) domains in the C* complex spliceosome (PDB 5MQF). In this model, the interaction with SYF1 and AQR is mediated through the PPI domain of PPIE rather than the RRM motif, and the model of U2 snRNA is placed extremely close to PPIE. In this structure the

orientation of the PPIE seems to be flipped, with the PPI domain interacting with AQR and SYF1, and the RRM motif close to PRPF17.

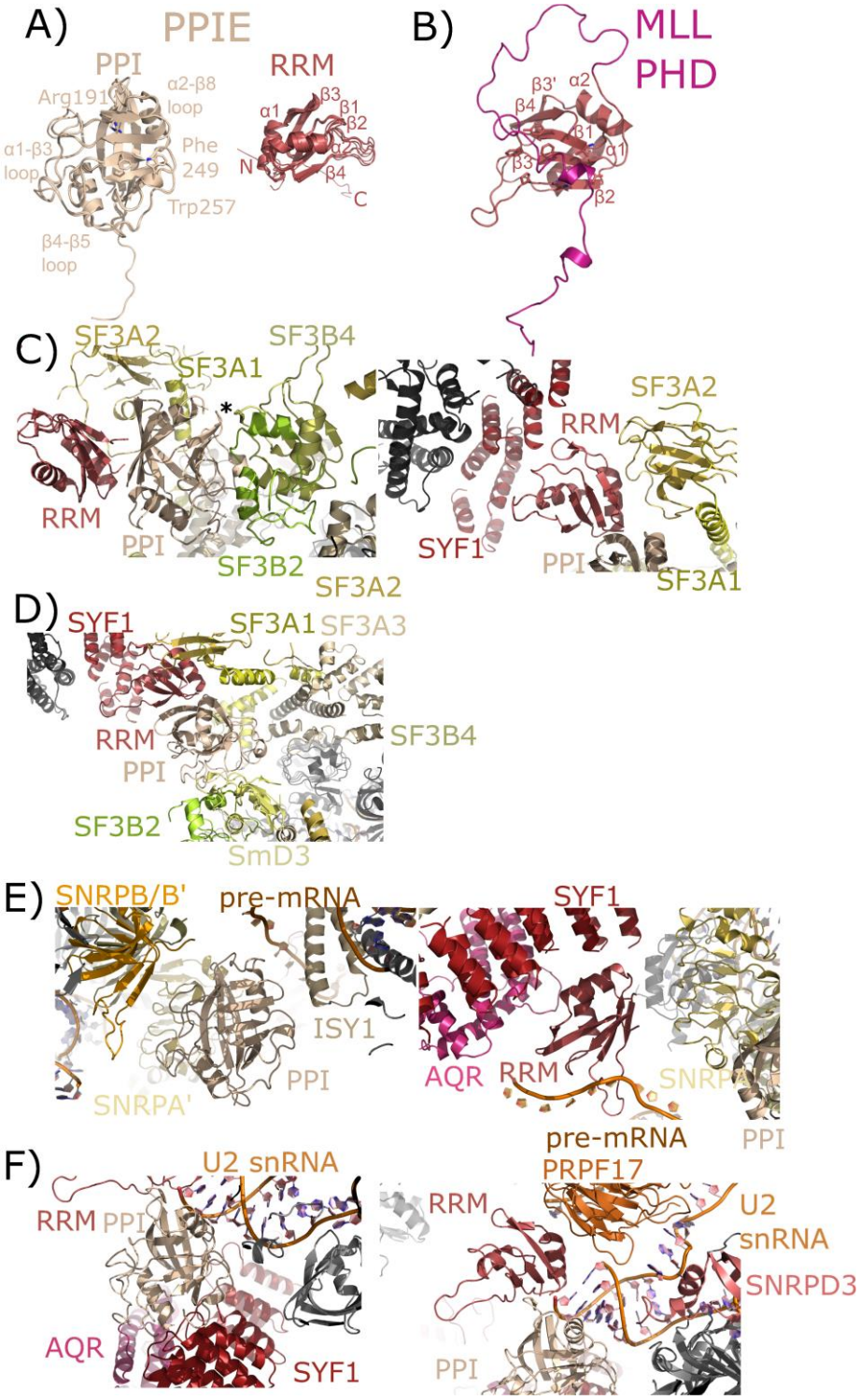

2.3. PPIL1

Peptidyl-prolyl isomerase-like isoform 1 (PPIL1) is a minimal cyclophilin, encoding for a single cyclophilin domain. The structure of PPIL1 was solved via NMR and initially described in [22]. Both Xu *et. al.* and a later study of PPIL1 was focused upon its interaction with the spliceosomal binding partner SNW1 (also known as SKIP, SKI-interacting protein) [21,22]. In these studies and others, the

interaction between PPIL1 and SNW1 was found to involve residues from the β2-α1, β4-β5, and β7-α2 loop regions outside of the S1 proline-binding pocket [15,21,22]. All these structures overlay nicely, considering they are derived from both crystallography and NMR (Figure 5A). PPIL1 has been assumed to regulate pre-mRNA splicing, as it has not been isolated as part of any other nuclear complex.

PPIL1 is an early spliceophilin; it is part of the PRP19 complex, along with SNW1. As with PPIE, PPIL1 is highly abundant in complex B* and complex B_{act} and is also abundant in the catalytic C complex [34,35]. Versions of complexes have been published out of *S. pombe* and human, but PPIE has only been visualized in human structures. PPIL1 is modeled in six deposited spliceosomal structures: the four outlined above that also contain PPIE, as well as an additional representative of B_{act} and C* complexes [23-28]. In the mature B_{act} complex, we again see interaction between the S1 pocket and proline, this time with proline 95 of PRPF17 (Figure 5B). All other interactions with PPIL1 are outside of the active site and include not only SNW1, but also RBM22 and SPF27 (Figure 5C). CDC5L and CRNKL1 are in the region, but not directly interacting with PPIL1. One novel finding within this spliceosomal structure is the extensive ordering of the disordered region of SNW1 around the β4-β5 and β7-α2 loop regions of PPIL1. All studies with isolated SNW1 polypeptides have been disordered, and so this is the first direct visualization of this interaction. In the B_{act} complex from Haselbach *et. al.*, many proteins seen in the mature B_{act} complex are missing from the model, and SNW1 is largely disordered (Figure 5D). However, the S1 interaction with PRPF17, and some of the previously described interactions with SNW1 and RBM22, are preserved. Finally, all three structures representing C complex are very similar, with PPIL1 interactions again with U5 snRNP40kDa, PRPF17, CDC5L, RBM22, CRNKL1, and SNW1. However, SYF2 is now interacting with the back-face of PPIL1 near α2 (Figure 5E).

Figure 5. Structures of PPIL1 in solution and in spliceosomes. In (A) PPIL1 is shown in cartoon representation (overlay of PDBs 1XWN, 2K7N, and 2X7K). Selected catalytic residues and protein:protein interaction regions are labeled, including the regions proposed to interact with SNW1 (SKIP) in solution. (B, C) PPIL1 in the "mature B_{act}" complex (PDB 5Z56). (B) The view from the catalytic face of PPIL1. Proline 95 from PRPF17, which is centered in the S1 pocket, is highlighted. (C) The view from the "back-face" of PPIL1. The interactions between PPIL1 and SNW1, RBM22, CRNKL1, and CDC5L are more clearly seen. Note the extensive ordering of the disordered region of SNW1 around the β4- β5 and β7-α2 loop of PPIL1. The PPIL1 region in the "late Bact" complex (PDB 5Z57) is identical to that of 5Z56, and is not shown here. (D) The PPIL1 neighborhood in the Bact complex (PDB 6FF4). While many of the interactions are similar to those shown in (B) and (C), many of the proteins seen in that complex are missing from this model. Left panel, the view from the catalytic face; right panel, the view from the back face. CRNKL1, CDC5L, and SPF27 are not modeled, and the ordered region of SNW1 is decreased. (E) The PPIL1 neighborhood in the C complex (PDB 5YZG) centered on the catalytic face (left) and the back-face (right). The PPIL1 interaction neighborhood is similar to that shown in (B) and (C) with the addition of the SYF2 protein to the model, which interacts with the back-face of PPIL1 near α2. The models of the C* in (PDB 5XJC) and (PDB 5MQF) is not shown, as the interaction environment around PPIL1 is very similar to that in (E).

Preprints (www.preprints.org) | NOT PEER-REVIEWED | Posted: 2 November 2018 doi:10.20944/preprints201811.0037.v1

Peer-reviewed version available at Biomolecules 2018, 8, 161; doi:10.3390/biom8040161

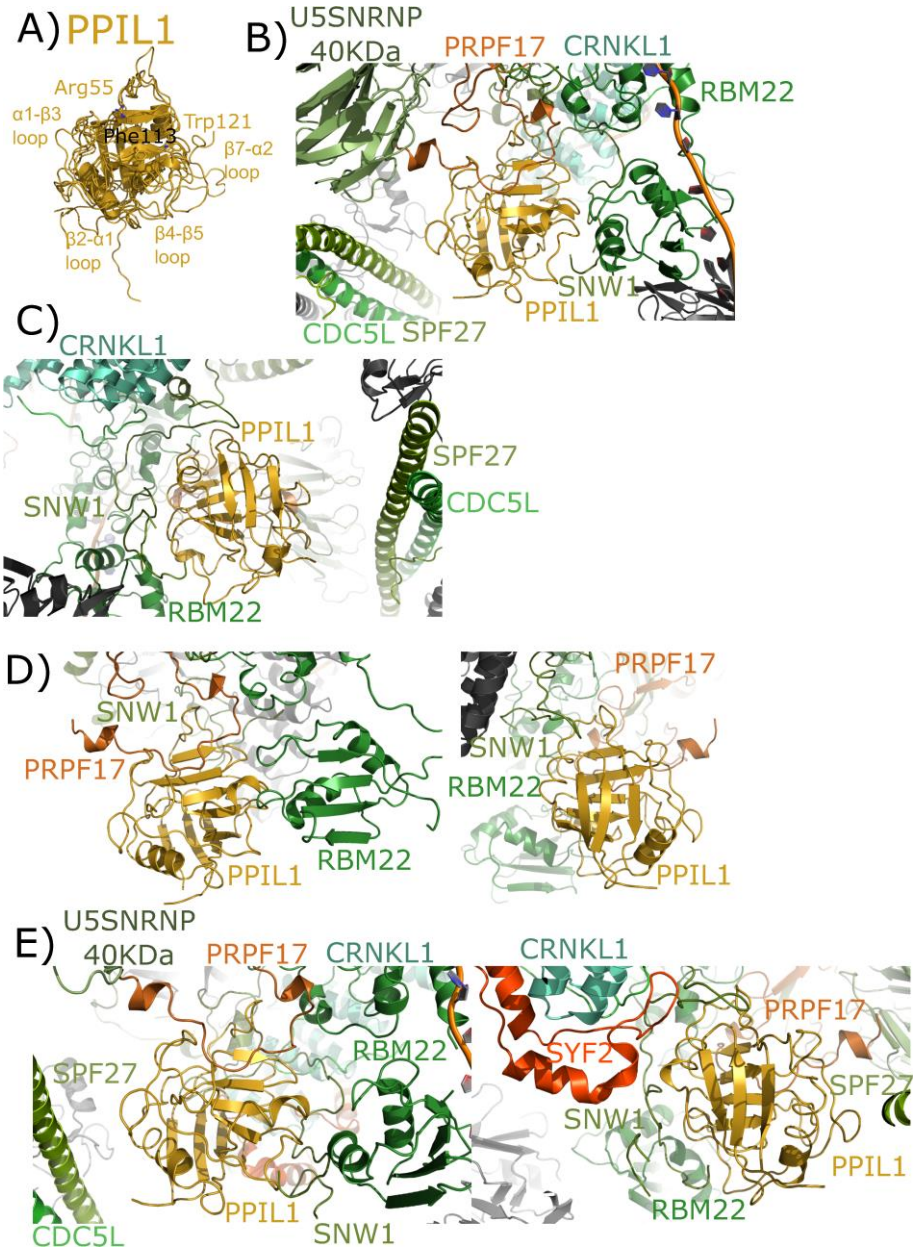

263

264

265 *2.4. PPIL2*

266 Peptidyl-prolyl isomerase-like isoform 2 (PPIL2) is a multi-domain cyclophilin, encoding for an
267 N-terminal Ubox-motif and a C-terminal cyclophilin domain (Figure 2). Aliases for PPIL2 include
268 Cyp-60, RING-Type E3 Ubiquitin Transferase Isomerase-Like 2, or UBOX7. The structure of the
269 cyclophilin domain of PPIL2 was solved at the SGC and published (Figure 6A) [2]. There is no
270 structure of the PPIL2 Ubox publicly available, although it is very similar to other Ubox motifs of the
271 C2H2 type, including the spliceosomal protein PRPF19 (Figure 6A). The Ubox of PPIL2 is active *in*
272 *vitro*, and has been reproducibly shown to perform as a functional E3 ligase when coupled to
273 ubiquitin, the canonical E1 UBA1, and a specific nuclear E2 (Figure 6B) ([46], TLD *unpublished data*).
274 No full-length structure of PPIL2 is available, and the physiological relevance of PPIL2's E3 ligase
275 activity remains unclear – although it is notable that splicing activity and the assembly of
276 spliceosomal complexes are likely regulated by ubiquitination [47-52]. PPIL2 is also part of a select
277 sub-set of spliceophilins with a naturally occurring substitution in the S1 pocket that renders it
278 incapable of prolyl isomerization, although still capable of binding proline. In PPIL2, the canonical
279 S1 residue Trp121 is replaced by a Tyr, resulting in a loss of both isomerase activity and affinity for

Preprints (www.preprints.org) | NOT PEER-REVIEWED | Posted: 2 November 2018 doi:10.20944/preprints201811.0037.v1

Peer-reviewed version available at Biomolecules 2018, 8, 161; doi:10.3390/biom8040161

the pan-inhibitor cyclosporine [2]. PPIL2 is an intermediate spliceophilin, part of a unique set of four proteins that associate transiently with the spliceosome during the transition from B_{act} to catalytic C complex [34,35]. As a consequence, PPIL2 is highly abundant only in B_{act}. Unsurprisingly, due to the highly transient nature of this sub-complex of the spliceosome, PPIL2 is not modeled in the existing structures of pre-catalytic spliceosomes.

PPIL2 has been proposed on the basis of pull-down and yeast two-hybrid data to interact with the spliceosomal proteins Zinc Finger 830 (ZNF830) and Papillary Renal Cell Carcinoma (PRCC) (available through the UniProtKB website) [53]. We have prepared soluble forms of full-length versions of both PPIL2 and ZNF830 proteins (Figure 6B). We have also isolated soluble forms of the two domains of ZNF830, along with the two domains of PPIL2. We then validated that full-length PPIL2 directly interacts with reasonable affinity (~500 nM) to full-length ZNF830 (Figure 6C). Interestingly, both the isolated Ubox motif and the cyclophilin domain of PPIL2 are able to mediate the interaction with ZNF830 (C. Rajiv, *unpublished thesis*). Additionally, we have evidence that both domains of PPIL2 simultaneously interact with ZNF830 (Figure 6D). Further work to delineate the functional significance of these interactions is ongoing, but certainly this mode of binding is unique among what we have seen for other spliceophilins.

Figure 6. Validation of interactions between PPIL2 and the spliceosomal protein ZNF830. In (A) PPIL2 is shown in cartoon representation (RCSB 1). Selected catalytic residues and protein:protein interaction regions are labeled. (B) PPIL2 is a functional E3 ligase. Increasing concentrations of PPIL2 in an *in vitro* assay and in the presence of ubiquitin, E1, and E2 proteins lead to the production of poly-Ub chains (TLD, *unpublished data*). (C) SPR of full-length PPIL2 (ligand) and ZNF830 (analyte) indicates nanomolar-affinity binding between the two proteins (C. Rajiv, *unpublished thesis*). (D) left panel, concentration dependence of isolated PPIL2 U-box binding to full-length ZNF830. Right panel, sequential addition of PPIL2 U-box followed by a mix of PPIL2 U-box and PPIL2 PPI domain results in increasing response upon ZNF830 ZnF. This is interpreted as an ability for both domains of PPIL2 to interact simultaneously with ZNF830 (C. Rajiv, *unpublished thesis*). Methods are summarized in Appendix A.

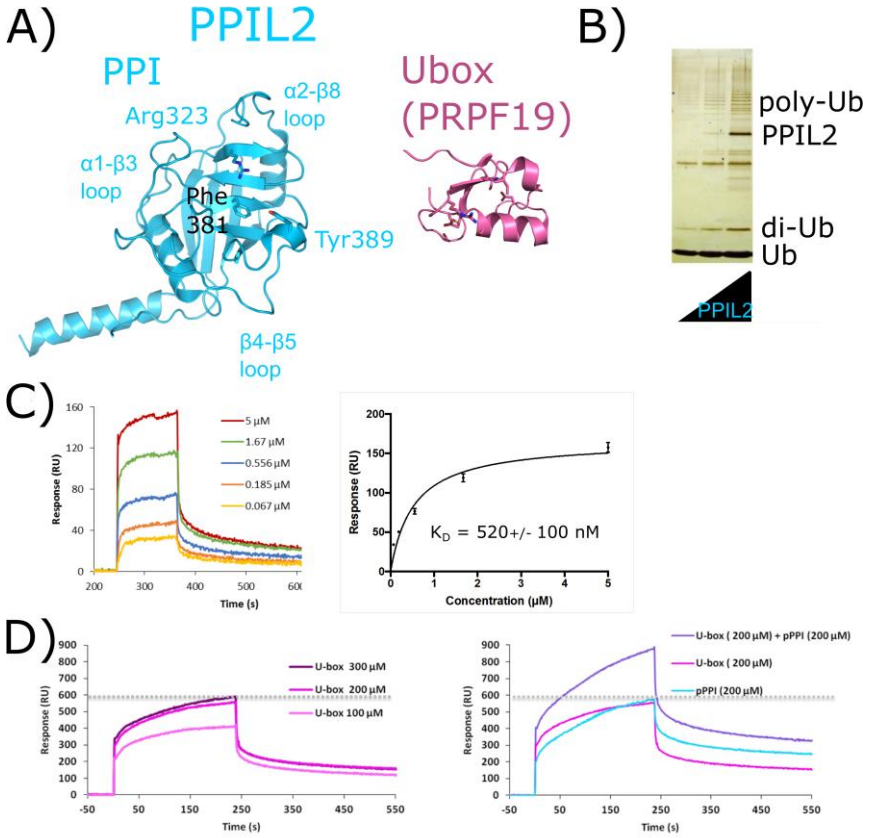

2.5. PPIL3

Peptidyl-prolyl isomerase-like isoform 3 (PPIL3) is a minimal cyclophilin. Initial studies called PPIL3 CypJ [54]. The structure of the cyclophilin domain of PPIL3 was solved via crystallography and initially described in [45]. A later structure of PPIL3 in apo form, and bound to cyclosporine, is also available in the RCSB (Chen *et. al.*, unpublished) (Figure 7A). PPIL3 is part of a group of spliceophilins, including PPIL2 and CWC27, which are first found in B_{act} complex. However, unlike PPIL2, PPIL3 is most abundant in C complex [34,35]. Although multiple cryo-EM structures of B_{act} and C complex exist, PPIL3 has not been successfully modeled into density.

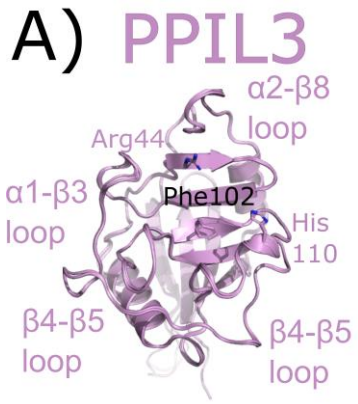

Figure 7. PPIL3 is shown in cartoon representation (RCSB 2XWN). Selected catalytic residues and protein:protein interaction regions are labeled.

2.6. CWC27

Variously called NY-CO-10, SDCCAG10, or SDCCAG-10, CWC27 is a complex cyclophilin, encoding for an N-terminal cyclophilin domain and a large C-terminal repetitive low complexity region of unknown function (Figure 2). The structure of the isolated cyclophilin domain of CWC27 was solved at the SGC, and was initially described in [2]. A later structural study of CWC27, comparing the human CWC27 to that of a thermophilic organism, can be found in [55]. Similarly to PPIL2, CWC27 is naturally substituted in the S1 pocket, with a glutamic acid substitution for tryptophan. Additionally, CWC27, like PPIL2 and PPIL3, is highly abundant in B_{act} complex, and is also found with moderate abundance in C complex [34,35].

The cyclophilin domain of CWC27 has been modeled into three spliceosomal complexes [23,25]. In the mature B_{act} complex, U5snRNP200kDa interacts with the α2-β8 region of CWC27; BUD31 is found near the β4- β5 loop; PRPF8 interacts with both the β4- β5 loop and β7-α2 region; and RNF113 interacts with the C-terminal linker region between the PPI and the low complexity region of CWC27, which is apparently disordered (Figure 8B). In the late B_{act} complex the CWC27 interaction environment is quite similar, save for the absence of BUD31 and slight movement of PRPF8 (Figure 8C). Finally, in the B_{act} complex of Haselbach *et. al.*, the modeled interactions are comparable. In this structure, more of RNF113 can be modeled in, including an additional, extensive interaction with β1-β2 of CWC27. BUD31 is included in the model, but U5 snRNP200kDa is not. Note that in all structures, only the cyclophilin domain of CWC27 can be modeled, leaving roughly 200 residues uncharacterized.

Preprints (www.preprints.org) | NOT PEER-REVIEWED | Posted: 2 November 2018 doi:10.20944/preprints201811.0037.v1

Peer-reviewed version available at Biomolecules 2018, 8, 161; doi:10.3390/biom8040161

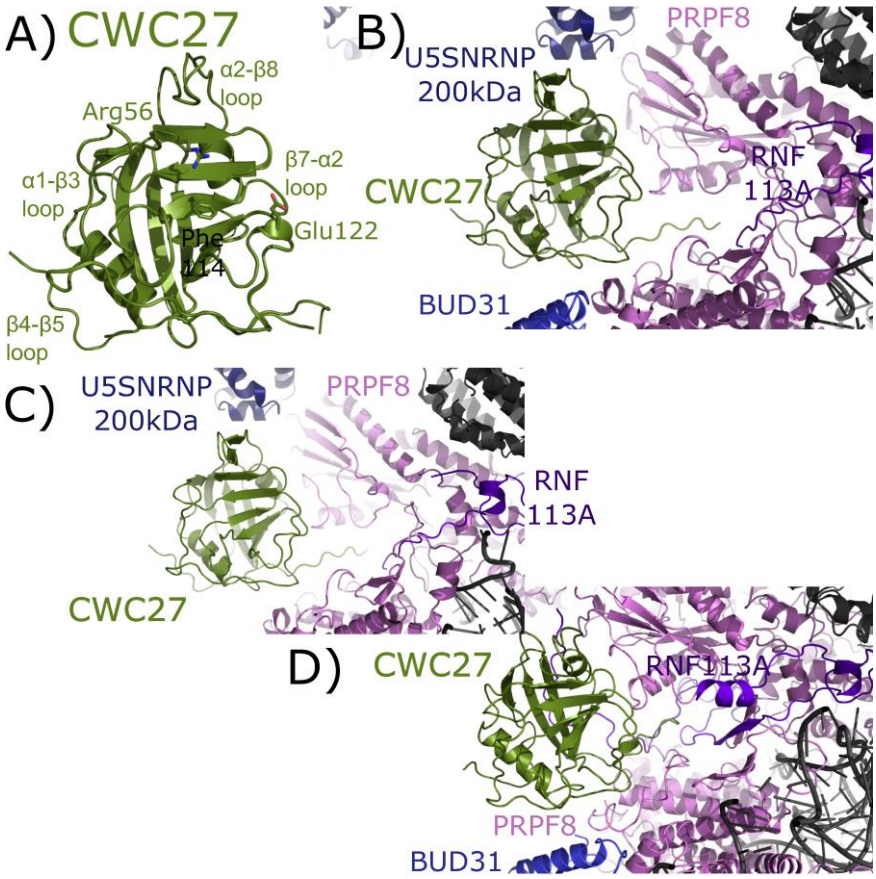

Figure 8. Structures of CWC27 in and out of the spliceosome. In (A) the cyclophilin domain of CWC27 is shown in cartoon representation (overlay of PDB 2HQ6 and 4R3E). Selected catalytic residues and protein:protein interaction regions are labeled. The substitution of Glu122 in the active site renders CWC27 inactive, although it still binds proline-containing pepetides. In (B) the neighborhood around the cyclophilin domain of CWC27 in the "mature" Bact complex (PDB 5Z56). Modeled interactions with U5 snRNP200kDa, BUD31, PRPF8, and RNF113 are highlighted. In (C), the neighborhood around CWC27 in the "late" Bact complex (PDB 5Z58). The view is very similar to that in PDB 5Z56, save for the absence of BUD31 and slight movement of PRPF8. In (D), the neighborhood around CWC27 in the Bact complex (PDB 6FF4) is shown. Again, the modeled interactions are very similar to those in (B) and (C), with more of RNF113 modeled in 6FF4, including an additional, extensive interaction with β1- β2 of CWC27. BUD31 is included in the model, but U5 snRNP200kDa is not. All models have only the cyclophilin domain of CWC27, with ~200 additional residues uncharacterized.

2.7. PPWD1

WD40-domain containing peptidyl-prolyl isomerase 1 (PPWD1) is a multi-domain cyclophilin, encoding for an N-terminal 7-bladed WD-40 domain and a C-terminal cyclophilin domain (Figure 2). An early alias of PPWD1, still found in some databases, is KIAA0073.The structure of the cyclophilin domain of PPWD1 was initially solved by the SGC, described in [2,19]. Interestingly, the crystal structure of the PPWD1 cyclophilin captured an interaction between molecules in the asymmetric unit that was proline-mediated; however, *in vitro* this isolated peptide was found to interact with PPWD1, but not to be a substrate for turnover (Figure 9B) [19]. We note that it is common in cyclophilin structures to find proline-containing peptides from symmetry-related cyclophilins interacting in the S1 pocket, and is perhaps one of the keys to both the crystallizability of these proteins, and their potential for higher-order aggregation in NMR studies (TLD, *personal communication*). PPWD1 is highly abundant only in C complex [34,35]. PPWD1 has been modeled in one structure of C complex [24]. In this complex, only PRPF8 is close enough to form contacts with the PPI domain of PPWD1, centered on the β7-α2 region. Over 90Å away, PRPF8 along with U5

snRNP200kDa form the neighborhood around the WD40 domain of PPWD1. This represents the first, and as of yet only, model of the WD40 domain of PPWD1.

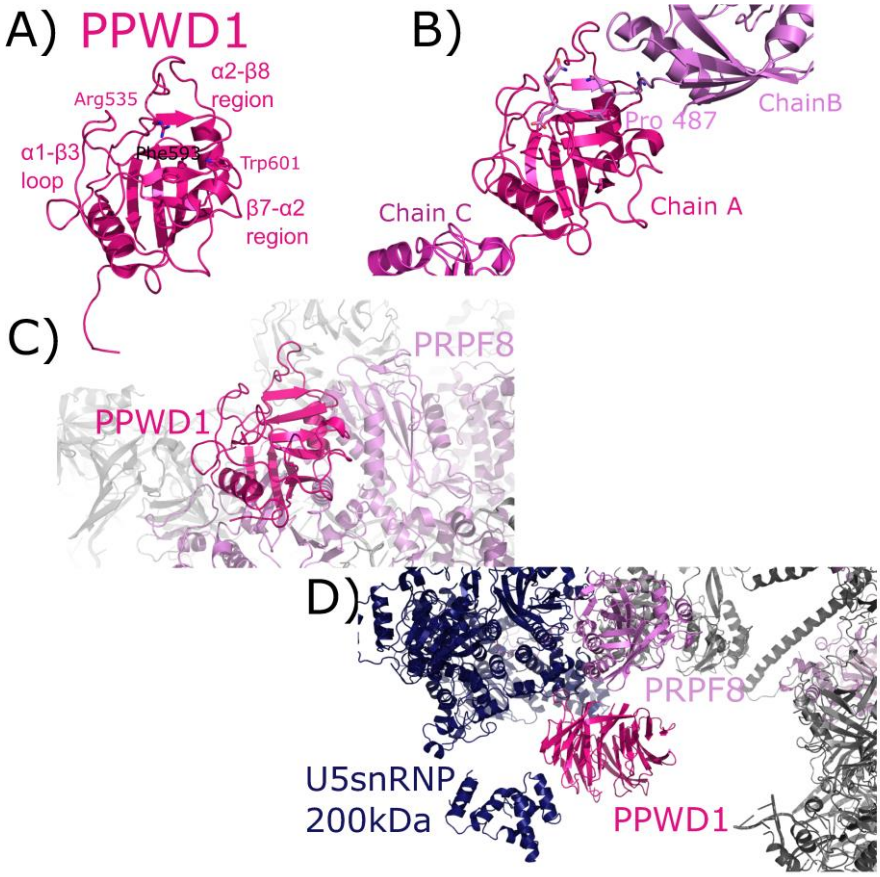

Figure 9. PPWD1 structures in and out of the spliceosome. In (A), one of the three molecules of the PPI domain of PPWD1 from the asymmetric unit of PDB 2A2N is shown in cartoon representation. Selected active site residues are labeled, along with the α1-β3 loop and the β7- α2 region. In (B), the view is expanded to include all three PPWD1 molecules in the asymmetric unit. The proline from a neighboring molecule is shown in the active site. Modified from []. In (C), the PPWD1 neighborhood is shown in the C complex (PDB 5YZG). Only PRPF8 is close enough to form contacts with the PPI domain of PPWD1. (D) Over 90Å away, PRPF8 along with U5 snRNP200kDa are modeled near the WD40 domain of PPWD1. For reference, the region of PRPF8 that interacts with the cyclophilin domain of PPWD1 is visible in the upper-right corner of the figure, in color. This represents the first, and as of yet only, model of the WD40 domain of PPWD1.

2.8. PPIG

Peptidyl-prolyl isomerase isoform G (PPIG) is a multi-domain cyclophilin. Much like NKTR, PPIG encodes for an N-terminal cyclophilin domain and a C-terminal SR-repeat region (Figure 2). Alias of PPIG include SR-Cyp or Clk-Associating RS-Cyclophilin (CARS-Cyp) [53].The structure of the cyclophilin domain of PPIG was solved at the SGC and was published (Davis, 2010). Later structures of the apo cyclophilin domain and bound to the pan-inhibitor cyclosporine were also published [56]. These structures are practically indistinguishable (Figure 10A). PPIG is not highly abundant in the spliceosome, but a small number of peptides were identified in C complex [34,35]. In spite of this, PPIG has been successfully modeled into one C complex structure [24]. In this structure, only the cyclophilin domain of PPIG is modeled, and it interacts with SNW1, modeled as an alpha helix and interacting in the α2-β8 loop region. PPIG is also seen to interact with CWC15 (β3-β4 loop), and PRPF8 (3_{10} helix). No model exists for the residues outside the PPIG cyclophilin domain, meaning roughly 600 residues of PPIG are unaccounted for in the structure.

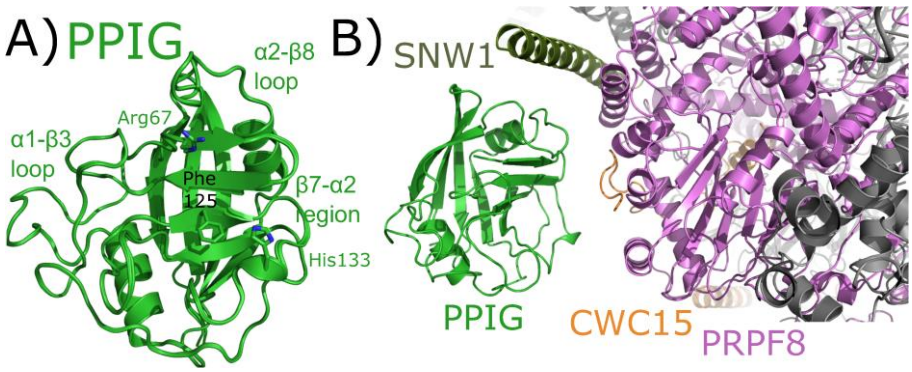

Figure 10. PPIG structures in and out of the spliceosomal context. In (A), the PPI domain of PPIG is shown in cartoon representation (overlay of PDB 2GW2, 2WFI, and 2WFJ). Selected residues in the catalytic site, along with regions of protein:protein interactions, are labeled. In (B), the neighborhood around the cyclophilin domain of PPIG in the catalytic C spliceosome (PDB 5YZG). Potential interactions between PPIG and SNW1, CWC15, and PRPF8 are highlighted. No model exists for the roughly 600 residues outside of the PPIG cyclophilin domain.

3. Structural Analysis of the Spliceophilins

Due to their soluble nature and ease of crystallization, the spliceophilins have been the targets of extensive biochemical and biophysical characterization. It is somewhat surprising how long it has taken to begin to visualize the protein and RNA neighbors of these proteins in the context of the spliceosome. Now that spliceosomal models exist that contain spliceophilins, what can we learn from these studies? First, it is useful to compare the numerous, publicly available results of proteomic studies to the protein neighbors of the spliceophilins depicted in Figures 3-10 above. PPIH, of course, was known to interact with PRPF4, and this interaction is preserved (Figure 3) [17,29,31,32]. On the other hand, PPIH is also found to interact with a whole host of other proteins, both spliceosomal and nuclear, along with cytosolic proteins, in major publicly available databases (BioGrid, IntAct, and STRING, all accessible through UniprotKB) [53]. In addition to PRPF4, which is represented in all three databases, there are interactions reported with other tri-SNRP components (PRPF3, PRPF8, PRPF18, PRPF31); with other spliceosome-associated proteins (hnRNPD, LSM4, LSM6, LSM8, BAG2); and with many other proteins that are seemingly unrelated to splicing complexes (USPs, Finbronectin-1, E3 ligases including HUWE1, etc.) [53]. How do we interpret these results, in the context of both extensive biochemical and structural work done on PPIH outside of the spliceosomal context, and also in the context of spliceosome structure? Firstly, many sub-complexes of the spliceosome, including the tri-sNRP, the PRP19 complex, and the IBC, are stable outside the context of the large spliceosome complex and may be isolated using pull-down or two-hybrid approaches [57-59]. Therefore, we must always keep in mind that the proteomics data in public databases are sensing not only single protein interactors but are detecting larger sub-complexes as well. Additionally, cyclophilins are very likely to provide both false positive and false negatives in proteomics studies, unless experimental conditions are optimized. This is because on the one hand, proline-mediated interactions and even native substrates of the cyclophilins tend to bind in the low-micromolar range of affinities. These are likely to go undetected in most proteomics screens, as evidenced by the PRPF4 interaction delineated in Rajiv *et. al.*, or the lack of any prior data indicating both PRPF17 and SF3A2 as a proline-mediated interactor of spliceophilins. On the other hand, interactions mediated by the α1-β3, β4-β5, and α2 region of spliceophilins seem, based on the limited amount of work reported, to provide much higher affinity binding sites for splicing complex proteins [17,21]. Generally, it seems like the cyclophilin fold can provide a productive set of surfaces centered on the extensive loop structures surrounding the beta-sandwich core, and these interactions may well be promiscuous. This is likely the reason why cytoplasmic proteins are seen to interact with nuclear spliceophilins, when they are unlikely to ever see these proteins in the cellular milieu. Even though several of these types of interactions may now been seen for the spliceophilins in splicing complexes, it is by no means sure that these interactions occur outside the scaffold of the full spliceosome, and it

Peer-reviewed version available at Biomolecules 2018, 8, 161; doi:10.3390/biom8040161

is also unlikely that the current spliceosomal structures contain all the potential interactions between spliceophilins and nuclear proteins that are possible. Without this full list of interactions, a consensus binding sequence to loop regions has to date been elusive, and not enough of these interactions have been biochemically characterized outside of the spliceosomal complex to allow for any predictive power to be applied as a filter to proteomics lists. Finally, a large degree of the diversity within spliceophilins is contained within modules outside of the cyclophilin domain. However, the relative challenges of expressing and purifying some of these domains (intrinsically disordered SR motifs and regions of low homology to other proteins, WD-40 domains) and the lack of domain-specific proteomic studies again slows progress along these lines. When they have been studied, either in the RRM domain of PPIE or the Ubox motif of PPIL2, these domains contribute additional functionality to the isomerase they are encoded with. Although recent structures of splicing complexes show us intriguing glimpses into the roles of the WD40 domain or the RRM motif in mediating spliceophilins interactions, the proteomics data does not discriminate between domain-specific interactions. Further work on isolated, purified proteins will be needed to truly understand the roles of the extra-isomerase domains on protein:protein interaction and/or function.

As an example of the limitations that all these concerns place upon the researcher studying protein:protein interactions with the spliceophilins, consider the case of PPIL2. PPIL2 is predicted to bind to proteins that we see binding to other spliceophilins, including CRNKL1, along with ZNF830 and PRCC, in multiple proteomics studies. Additionally, by constructing a family of constructs to parse out domain and full-length protein:protein interactions, we have shown *in vitro* that PPIL2 interacts at a minimum with ZNF830, yielding both a quantitative validation of proteomics data, and an interesting and complex study of two multi-domain proteins in solution. However, without visualization of PPIL2 and ZNF830 within the spliceosomal sub-complex they both participate in, we cannot say with certainty that the data being generated from these other experimental sources are indeed relevant to spliceosome biology. Similarly, proteomics-derived data for PPIL3 will not be described here, as it has not yet been validated by either *in vitro* approaches, nor visualized in spliceosome structure.

On the other hand, there are several cases presented in this review in which splicing complexes are providing the first independent validation of predicted interactions with spliceophilins. For PPIE, SF3B4 is indicated for the first time to be a proline-mediated interactor through the S1 pocket. SF3B2, SF3A2, SNRNP A', B/B', and SmD3 all interact with the PPI domain of PPIE. These structures are also able to isolate PPI interactions form those of RRM, with the RRM interacting with SF3A2, SYF1, AQR, and pre-mRNA substrate can be added to the list of PPIE interactions. All of these interactions are found within BIOGRID, along with many others (CDC5L, SNW1, PRPF8, XAB2, etc.). As both the RRM and PPI domains of PPIE are quite soluble and well-behaved in solution, perhaps the spliceosome structures will provide the impetus needed to drive further research into validation of these interactions individually *in vitro*. As this is the only spliceophilin seen interacting directly with pre-mRNA substrate, it is hoped that further work to identify the potential role of PPIE in regulating alternative or constitutive splicing in vivo will be inspired by this structure. PPIL1 is seen to interact with PRPF17 through S1. SNW1, CRNKL1, RBM22, CDC5L, U5 snRNP40kDa, and SYF2 are all seen to be interactors with PPIL1, vastly expanding the potential interaction repertoire of this minimal spliceophilin. Save for SNW1, most of these interactions are not contained within BIOGRID or STRING, except for CDC5L. This highlights the importance of complementary approaches to obtain information about these protein:protein interactions within subcomplexes, such as the PRP19 complex. CWC27 interacts with U5 snRNP200kDa, BUD31, PRPF8, and RNF113. It is interesting that CWC27, which is not an active isomerase like PPIE and PPIL1, is not seen interacting with protein in the S1 pocket (although, as noted above, negative results cannot be conclusive due to the poor affinity proline-containing substrates have for both active isomerases, and even more so for substituted S1 sites). None of these interactions were pulled out from STRING or BIOGRID, at least not as direct interactions with CWC27. It is unfortunate that the low-complexity regions of CWC27 could not be modeled in structure, but many new hypotheses can be derived and tested from the current structural data, which is quite exciting. We find PPWD1 interacting with PRPF8 through both its PPI and WD40

Peer-reviewed version available at Biomolecules 2018, 8, 161; doi:10.3390/biom8040161

domains, which also interacts with U5 snRNP200kDa. These interactions have not been captured in BIOGRID or STRING, again generating new possibilities for functional and/or structural work. We note especially the power of visualizing the WD40 domain of PPWD1 in the spliceosome, as this isolated domain is historically extremely difficult to express and purify *in vitro*. Finally, PPIG interacts with SNW1, CWC15, and PRPF8, all through the PPI domain. None of these interactions are in BIOGRID or STING. The SR region of PPIG is not modeled, unfortunately; this region, which should be a hotspot for regulation of alternative splicing through SRPKs, would have been extremely interesting to visualize, and is not likely to be ordered or properly post-translationally modified using *in vitro* purified protein.

Finally, two useful analyses to perform across all spliceosome structures are to look at the interactors seen to bind to spliceophilins over all structures. We see interactions through the S1 pocket by SF3B4 and PRPF17, and many interactions with the loop structures of the various spliceophilins. However, there are a few spliceosomal proteins that occur in multiple structures, interacting with multiple spliceophilins. Of particular note is the central splicing regulator PRPF8, which is in close proximity to four spliceophilin PPI domains: PPWD1, CWC27, PPIG, and PPIH. This speaks indirectly to the central importance of the spliceophilins family in proper spliceosome function, and merits further research. Another interesting note is to compare the spliceophilins themselves. The structural similarity of the cyclophilin domain confounds researchers attempting to predict potential unique binding partners within the nucleus – across the eight nuclear cyclophilins, structural alignments result in an overall RMSD of less than 2Å [2]. More importantly, it has become clear over the last 10 years in this field that the active site for prolyl isomerization is not the only, nor perhaps the major, site of protein:protein interactions with the spliceophilins [15,17,21,33,53]. One obvious outcome from the splicing complexes released to date is that we still do not understand how S1 interactions with proline-containing substrates are driven, at least in any way that could be predictive. There is no other corroborating evidence linking PRPF17 or SF3B4 as substrates for proline turnover, and yet the data from the spliceosome structures of mature B_{act} is quite convincing. Other than for PPIL2 or CWC27, in which the active site is substituted in such a way as to lose affinity for proline, we cannot see any differences between the S1 sites of spliceophilins that would preclude interactions with prolines, and there are thousands of proline-containing peptides in spliceosomal proteins [47]. It remains to be seen what the consequences of these interactions are, or under what conditions they can be studied *in vitro*. However, the mere presence of these interactions within B_{act} represent a wealth of information for cyclophilin researchers. Likewise, based on this collection of structures it seems that some spliceophilins are more promiscuous in their loop region interactions than others. In particular the early spliceophilins PPIE and PPIL1 participate in a complicated and large protein network within pre-catalytic and catalytic complexes, while others (PPIG, PPIH, and PPWD1) are interacting with only one or two other proteins. As mentioned previously, one must be careful over-analyzing negative results in these structures, as disorder or dynamic heterogeneity may result in the inability to model protein or RNA into structure; however, from what we currently know, it seems that certain spliceophilins may be more "connected" in structure than others. What effect this may have on their biological function within splicing complexes is an exciting and largely un-addressed question which these structures may help to inspire.

4. Spliceophilin Function

It is important to consider what is known (or supposed) about the cellular role of the cyclophilins in biological function before considering rational drug design against this family of enzymes. With at least 18 family members in human cells, most ubiquitously expressed across tissues and throughout development and into adult, finding unambiguous biological effects due to a specific cyclophilin is difficult. The high degree of conservation in the active site of these proteins does not often allow for substrate proline prediction, and in the cases where biologically relevant substrates have been identified, it is often due to specific localization of a single or sub-set of cyclophilins away from the rest. For instance, in the identification of the secreted cyclophilins (PPIA, PPIB, PPIC) as interacting viral proteins, a critical determinant of specificity was the fact that these cyclophilins were

Preprints (www.preprints.org) | NOT PEER-REVIEWED | Posted: 2 November 2018 doi:10.20944/preprints201811.0037.v1

Peer-reviewed version available at Biomolecules 2018, 8, 161; doi:10.3390/biom8040161

the only ones that could reasonably be expected to be found outside of the cell. Likewise, the wealth of research identifying PPIF as a mediator of mitochondrial function, and therefore a viable drug target to modulate same, benefitted from the fact that there is only one possible cyclophilin candidate in mitochondria. The identification of specific nuclear cyclophilins as spliceophilins, and later assignment to specific cyclophilins to specific sub-complexes throughout the splice cycle, may well provide another opportunity to assign specific effects to individual cyclophilins. A spliceosome-wide approach using siRNA pools found that the spliceophilins, and specifically the early spliceophilin PPIH, was actively participating in regulating the splicing of targets in apoptosis and inflammation [60,61]. We wished to see transcriptome-wide effects on splicing, and created stably transfected knockdown human cell lines, validated for significant knockdown of each of the eight spliceophilins. We have completed splicing microarrays for each knockdown, and can say that removing individual spliceophilins from cells results in large changes in thousands of splicing events (Figure 11A and 11B; see Accession Codes section for deposited GEO accession codes). We see, as in Papasaikas, *et. al.*, that when a sub-set of regulated splicing events are selected for analysis, there are certain spliceophilins that seem to exert greater regulatory control for others. In both our hands, we find that PPIH is a "master regulator" of alternative splicing; we also find that PPIL2 is in the same class, at least for the sub-set of splicing events and spliceophilins we studied (Figure 11C) [61]. By transiently transfecting expression constructs of cyclophilin domains into these stable lines, we can identify which splicing events are regulated more directly, over shorter timeframes; and by transfecting in PPI domains with null mutations, we can assign events to isomerase activity (Figure 11B). Generally, what we see for the spliceophilins corroborates the models that we have generated from our *in vitro* studies; it is interactions outside the active site of the spliceophilins that largely dictate their ability to modulate splicing, not their isomerase activity per se (Figure 11B). On the other hand, we have seen several cases in which the isomerase activity of the spliceophilin is indeed dictating function; surprisingly, all of these effects to date have been on transcriptional targets (TLD, *data not shown*). This was supported recently by an elegant study delineating the role of a sub-set of nuclear cyclophilins in directly interacting with the transcription factor BMAL and regulating circadian rhythm in cells [18]. We feel this is likely to be a more general mechanism; taken together, the effect of cyclophilins in the nucleus is to directly (through interaction with transcription factors) or indirectly (through chromatin) regulate transcription, and to indirectly modify alternative splicing through participation in splicing complexes mainly through interactions outside of the S1 pocket. Much work remains to be done on the biological function of spliceophilins within alternative splicing; this work will only benefit by the insights provided by spliceosomal structures and could also greatly benefit from increased effort to design splicing modulators that target spliceophilins.

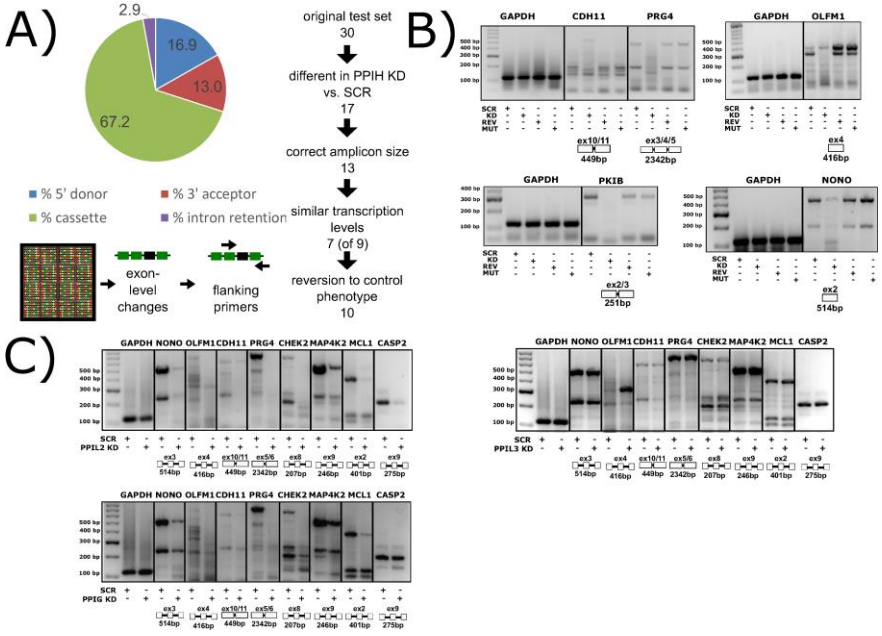

Figure 11. Spliceophilins impact alternative splicing patterns in human cells. (A) Knockdown of PPIH using RNAi results in changes in cassette exon, 5′ and 5′ splice sites, and intron retention, as measured by the HTA2.0 Affymatrix array. (B) Compared to control cells (SCR), PPIH knockdown cells (KD) exhibit altered alternative splicing of multiple genes (labeled at top of gels). Methods are summarized in Appendix B. When full-length PPIH is transiently expressed in knockdown cells (REV), the splicing changes are reversed. When the W133A mutant of PPIH (MUT) is transiently expressed, the KD phenotype is seen, indicating that isomerase activity is dispensable for this function. (C) PPIL2 KD exhibits splicing patterns identical to that of PPIH knockdown, while PPIG only regulates a sub-set of genes, and PPIL3 does not regulate any of the common targets tested. Not shown, PPIH KD regulates all splicing events tested to date. All panels from (Nii Martey, *unpublished data*). Methods are summarized in Appendix B.

5. Spliceophilins: Highly Druggable Modulators of Nuclear Function?

It is worthwhile to discuss the state of the field as regards rational drug design to obtain isoform-selective cyclophilin inhibitors. For many years, the pan-inhibitor cyclosporine was the only available option to researchers to study cyclophilin activity *in vitro* or function in vivo; solubility issues and broad, potent inhibition of most cyclophilin family members presented many barriers to insight. The alternative scaffold of sanghliferin and later scaffolds have presented similar issues, often without impressive increase in selectivity. Most drug development has focused on the connection between secreted cyclophilins and infectious disease, or to the identification of PPIF as a modulator of the mitochondrial permeability transition pore complex [5,6,62]. The majority of this work continues to target the S1 pocket; highly conserved and extremely accessible to solvent, this approach is nearly guaranteed to generate pan-inhibitors with significant off-target activity [10,63,64]. In 2010, we published a study in which we identified and characterized a site contiguous to S1. This site, the S2 region, is much less well conserved across the cyclophilin family, and importantly there is often little or no conservation in S2 for cyclophilins localized to the same compartment of the cell [2]. A study published in 2016 was the first to use this analysis of S2 as a basis for the rational design of drug-like compounds, targeting PPIF [10]. The S2 approach seems primed to provide cyclophilin researchers with valuable pharmacophores to tease out the functional roles of individual cyclophilins in cells. The exponential growth of available spliceosomal complex structures, along with the incremental work helping to define spliceophilins as regulators of both splicing and transcription, presents a novel opportunity for research. Developing S2-selective pharmacophores to modulate alternative splicing, chromatin regulation, and transcriptional activity by spliceophilins could benefit both basic and translational research. If S2 targeting continues to be successful and is implemented in a systemic way to the spliceophilins sub-family, we may well be on the cusp of a new era of research into this complex, intriguing, and important class of human proteins.

6. Conclusions and Final Thoughts

The advent and proliferation of published cryo-EM structures of the spliceosome might have been expected to yield great structure-based insight into the spliceophilins. Indeed, a whole host of novel, hypothesis-generating observations can be made based on the models released to the public. It is interesting at this stage of spliceosomal research to review the unforeseen reasons these studies have not yet delivered completely on their great promise for those in the cyclophilin field. In all structures reported to date, a majority of the appropriate spliceophilins are retained during purification, as evidenced by mass spectroscopy; however, even when binding partners are partially visible, no clear density for the spliceophilin is seen. Although the cyclophilins are highly structured with very little conformational dynamics on long timescales, they participate in highly dynamic interactions within the spliceosome. Whether these conformational dynamics are imparted by cyclophilins interacting directly with intrinsically disordered proteins (in the cases of PPIL1 and SNW1, or PPIH and PRPF4); because the nature of peptidyl-prolyl isomerase activity is to impart

greater conformational heterogeneity in the region surrounding the target proline; or whether it is because spliceophilins tend to be found on the more dynamic periphery of the spliceosome, the effect is to make regions of the spliceosome containing cyclophilins more difficult to capture and visualize using structural methods. When these regions can be accurately modeled, they are providing great insight into the nature of the interactions between spliceophilins and their physiologically relevant binding partners; we await with great excitement future structures, which we expect will provide only more fruitful data for hypothesis generation in this field. Structural biologists have always led the way in studying the family of human cyclophilins and have consistently driven the conversation about cyclophilin function into new and interesting areas of research. Smaller studies on individual spliceophilins complexed with one or two binding partners remains the most tractable system for studying both orthosteric and allosteric interactions in higher resolution and on shorter timescales, but larger-scale structural work on spliceosomes and other nuclear complexes can also provide important insights. Working together with cell biologists to find the direct and indirect molecular targets of spliceophilin function in the nucleus, and chemists to design effective small molecules targeting the spliceophilins, will drive forward research into this intriguing, challenging, and rewarding field.

7. Accession Codes

Accession Codes for the cyclophilins described in this manuscript (UniProt AC): PPIA (P62937), PPIH (O43447), PPIE (Q9UNP9), PPIL1 (Q9Y3C6), PPIL2 (Q13356), PPIL3 (Q9H2H8), CWC27 (Q6UX04), PPWD1 (Q96BP3), and PPIG (Q13427). GEO accession numbers for splicing microarray data resulting from knockdown of nuclear cyclophilins compared to scramble controls are: PPIH (GSE103648), PPIE (GSE117178), PPIL1 (GSE117381), PPIL2 (GSE117373), PPIL3 (GSE117302), CWC27 (GSE117144), PPWD1 (GSE117376), and PPIG (GSE117234).

Supplementary Materials: The following are available online, Supplemental Table S1: bioinformatics, Supplemental Table S2: spliceosome data.

Author Contributions: CR and TLD initiated ideas for the review, and contributed to figures and writing. TLD was responsible for editing.

Funding: TLD, and the data presented in Figures 6 and 11, was supported by funding from the National Institutes of General Medical Sciences [R00GM094293]. The content is solely the responsibility of the authors and does not necessarily represent the official views of the National Institute of General Medical Sciences or the National Institutes of Health.

Acknowledgments: The authors would like to acknowledge the contributions of the members of DavisLab, much of which could not be included in this review. Nii Martey Armah, Jessica Thorpe, and Jessica Kopenhaver of Drexel University contributed to the experiments presented in Figure 11.

Conflicts of Interest: The authors declare no conflict of interest.

Appendix A

Three constructs of ZNF830 were purified: full-length protein (aa 1-372), ZNF domain (1-90), and DUF domain (299-372) were cloned into pet15-MHL, an N-terminal cleavable $(His)_6$ tag (EF456738). The same vector was used to express full-length, U-box, and PPI domain of PPIL2. PPIL2 constructs were a generous gift from the SGC. Proteins were expressed in *E.coli* and purified using IMAC and SEC as described in [2] and [17]. Proteins were dialyzed into SPR buffer (20 mM Tris pH

8, 150 mM NaCl, 1 mM EDTA8, and 5mM β-ME) before use. SPR was performed using the ProteONXPR system and GLC chips, both from Bio-Rad.

Appendix B

Clones from the MISSION® TRC-Hs Human libraries were used to create stable knockdown lines in human cells (HEK293T except for PPIH, in HeLa). 2-5 sequences of shRNA were tested to ensure acceptable knockdown of mRNA and protein (60% KD or greater). cDNA from triplicate samples of PPIH knockdown were submitted for microarray analysis using the GeneChip® Human Transcriptome Array 2.0 (HTA 2.0), along with triplicate samples of scramble shRNA-containing cell lines. Microarray data were processed using TAC (Transcriptome Analysis Console) software to find significant splicing-level events. Validation was performed by designing primers for PCR that flanked each event as indicated in the microarray. Primers were designed to amplify the potential splicing event in as many annotated splicing isoforms in BLAST as possible. Standard PCR was performed, and resulting amplicons assayed in a 3% agarose gel. GAPDH was used as a loading control, to ensure that approximately equal amounts of cDNA had been loaded in each PCR reaction.

References

1. **Ferreira, P.A.; Orry, A. From Drosophila to humans: reflections on the roles of the prolyl isomerases and chaperones, cyclophilins, in cell function and disease. *J Neurogenet* 2012, *26*, 132-143, doi:10.3109/01677063.2011.647143.**

2. **Davis, T.L.; Walker, J.R.; Campagna-Slater, V.; Finerty, P.J.; Paramanathan, R.; Bernstein, G.; MacKenzie, F.; Tempel, W.; Ouyang, H.; Lee, W.H., et al. Structural and Biochemical Characterization of the Human Cyclophilin Family of Peptidyl-Prolyl Isomerases. *PLoS Biology* 2010, *8*, e1000439-e1000439.**

3. **Galat, A. Peptidylproline cis-trans-isomerases: immunophilins. *European Journal of Biochemistry / FEBS* 1993, *216*, 689-707.**

4. **Kumari, S.; Roy, S.; Singh, P.; Singla-Pareek, S.L.; Pareek, A. Cyclophilins: proteins in search of function. *Plant Signal Behav* 2013, *8*, e22734.**

5. **Valasani, K.R.; Sun, Q.; Fang, D.; Zhang, Z.; Yu, Q.; Guo, Y.; Li, J.; Roy, A.; ShiDu Yan, S. Identification of a Small Molecule Cyclophilin D Inhibitor for Rescuing Abeta-Mediated Mitochondrial Dysfunction. *ACS Med Chem Lett* 2016, *7*, 294-299.**

6. **Shore, E.R.; Awais, M.; Kershaw, N.M.; Gibson, R.R.; Pandalaneni, S.; Latawiec, D.; Wen, L.; Javed, M.A.; Criddle, D.N.; Berry, N., et al. Small Molecule Inhibitors of Cyclophilin D To Protect Mitochondrial Function as a Potential Treatment for Acute Pancreatitis. *J Med Chem* 2016, *59*, 2596-2611, doi:10.1021/acs.jmedchem.5b01801.**

7. **Gordan, R.; Fefelova, N.; Gwathmey, J.K.; Xie, L.H. Involvement of mitochondrial permeability transition pore (mPTP) in cardiac arrhythmias: Evidence from cyclophilin D knockout mice. *Cell Calcium* 2016, 10.1016/j.ceca.2016.09.001, doi:10.1016/j.ceca.2016.09.001.**

8. **Yoshikawa, R.; Izumi, T.; Nakano, Y.; Yamada, E.; Moriwaki, M.; Misawa, N.; Ren, F.; Kobayashi, T.; Koyanagi, Y.; Sato, K. Small ruminant lentiviral Vif proteins commonly utilize cyclophilin A, an evolutionarily and structurally conserved protein, to degrade ovine and caprine APOBEC3 proteins. *Microbiol Immunol* 2016, *60*, 427-436, doi:10.1111/1348-0421.12387.**

9. Dawar, F.U.; Tu, J.; Khattak, M.N.; Mei, J.; Lin, L. Cyclophilin A: A Key Factor in Virus Replication and Potential Target for Anti-viral Therapy. *Curr Issues Mol Biol* 2016, *21*, 1-20.

10. Ahmed-Belkacem, A.; Colliandre, L.; Ahnou, N.; Nevers, Q.; Gelin, M.; Bessin, Y.; Brillet, R.; Cala, O.; Douguet, D.; Bourguet, W., et al. Fragment-based discovery of a new family of non-peptidic small-molecule cyclophilin inhibitors with potent antiviral activities. *Nature Communications* 2016, *7*, 12777.

11. Kallen, J.; Mikol, V.; Taylor, P.; D Walkinshaw, M. X-ray structures and analysis of 11 cyclosporin derivatives complexed with cyclophilin A1. *Journal of molecular biology* 1998, *283*, 435-449.

12. Kallen, J.; Walkinshaw, M.D. The X-ray structure of a tetrapeptide bound to the active site of human cyclophilin A. *FEBS Letters* 1992, *300*, 286-290.

13. Kallen, J.; Spitzfaden, C.; Zurini, M.G.; Wider, G.; Widmer, H.; Wüthrich, K.; Walkinshaw, M.D. Structure of human cyclophilin and its binding site for cyclosporin A determined by X-ray crystallography and NMR spectroscopy. *Nature* 1991, *353*, 276-279.

14. Ke, H.M.; Zydowsky, L.D.; Liu, J.; Walsh, C.T. Crystal structure of recombinant human T-cell cyclophilin A at 2.5 A resolution. *Proc Natl Acad Sci U S A* 1991, *88*, 9483-9487.

15. Stegmann, C.M.; Luhrmann, R.; Wahl, M.C. The crystal structure of PPIL1 bound to cyclosporine A suggests a binding mode for a linear epitope of the SKIP protein. *PLoS ONE* 2010, *5*, e10013, doi:10.1371/journal.pone.0010013.

16. Adams, B.M.; Coates, M.N.; Jackson, S.R.; Jurica, M.S.; Davis, T.L. Nuclear cyclophilins affect spliceosome assembly and function *in vitro*. *Biochem J* 2015, *469*, 223-233, doi:10.1042/BJ20150396.

17. Rajiv, C.; Jackson, S.R.; Cocklin, S.; Eisenmesser, E.Z.; Davis, T.L. The spliceosomal proteins PPIH and PRPF4 exhibit bi-partite binding. *Biochem J* 2017, *474*, 3689-3704, doi:10.1042/BCJ20170366.

18. Gustafson, C.L.; Parsley, N.C.; Asimgil, H.; Lee, H.W.; Ahlbach, C.; Michael, A.K.; Xu, H.; Williams, O.L.; Davis, T.L.; Liu, A.C., et al. A Slow Conformational Switch in the BMAL1 Transactivation Domain Modulates Circadian Rhythms. *Mol Cell* 2017, *66*, 447-457 e447, doi:10.1016/j.molcel.2017.04.011.

19. Davis, T.L.; Walker, J.R.; Ouyang, H.; MacKenzie, F.; Butler-Cole, C.; Newman, E.M.; Eisenmesser, E.Z.; Dhe-Paganon, S. The crystal structure of human WD40 repeat-containing peptidylprolyl isomerase (PPWD1). *FEBS J* 2008, *275*, 2283-2295, doi:10.1111/j.1742-4658.2008.06381.x.

20. Skruzný, M.; Ambrozková, M.; Fuková, I.; Martínková, K.; Blahůsková, A.; Hamplová, L.; Půta, F.; Folk, P. Cyclophilins of a novel subfamily interact with SNW/SKIP coregulator in Dictyostelium discoideum and Schizosaccharomyces pombe. *Biochimica Et Biophysica Acta* 2001, *1521*, 146-151.

21. Wang, X.; Zhang, S.; Zhang, J.; Huang, X.; Xu, C.; Wang, W.; Liu, Z.; Wu, J.; Shi, Y. A Large Intrinsically Disordered Region in SKIP and Its Disorder-Order Transition Induced by PPIL1 Binding Revealed by NMR. *Journal of Biological Chemistry* 2009, *285*, 4951-4963.

22. Xu, C. Solution Structure of Human Peptidyl Prolyl Isomerase-like Protein 1 and Insights into Its Interaction with SKIP. *Journal of Biological Chemistry* 2006, *281*, 15900-15908.

23. Zhang, X.; Yan, C.; Zhan, X.; Li, L.; Lei, J.; Shi, Y. Structure of the human activated spliceosome in three conformational states. *Cell Res* 2018, *28*, 307-322, doi:10.1038/cr.2018.14.

24. Zhan, X.; Yan, C.; Zhang, X.; Lei, J.; Shi, Y. Structure of a human catalytic step I spliceosome. *Science* 2018, *359*, 537-545, doi:10.1126/science.aar6401.

25. Haselbach, D.; Komarov, I.; Agafonov, D.E.; Hartmuth, K.; Graf, B.; Dybkov, O.; Urlaub, H.; Kastner, B.; Luhrmann, R.; Stark, H. Structure and Conformational Dynamics of the Human Spliceosomal B(act) Complex. *Cell* 2018, *172*, 454-464 e411, doi:10.1016/j.cell.2018.01.010.

26. Zhang, X.; Yan, C.; Hang, J.; Finci, L.I.; Lei, J.; Shi, Y. An Atomic Structure of the Human Spliceosome. *Cell* 2017, *169*, 918-929 e914, doi:10.1016/j.cell.2017.04.033.

27. Bertram, K.; Agafonov, D.E.; Liu, W.T.; Dybkov, O.; Will, C.L.; Hartmuth, K.; Urlaub, H.; Kastner, B.; Stark, H.; Luhrmann, R. Cryo-EM structure of a human spliceosome activated for step 2 of splicing. *Nature* 2017, *542*, 318-323, doi:10.1038/nature21079.

28. Bertram, K.; Agafonov, D.E.; Dybkov, O.; Haselbach, D.; Leelaram, M.N.; Will, C.L.; Urlaub, H.; Kastner, B.; Luhrmann, R.; Stark, H. Cryo-EM Structure of a Pre-catalytic Human Spliceosome Primed for Activation. *Cell* 2017, *170*, 701-713 e711, doi:10.1016/j.cell.2017.07.011.

29. Horowitz, D.S.; Lee, E.J.; Mabon, S.A.; Misteli, T. A cyclophilin functions in pre-mRNA splicing. *The EMBO Journal* 2002, *21*, 470-480.

30. Teigelkamp, S.; Achsel, T.; Mundt, C.; Göthel, S.F.; Cronshagen, U.; Lane, W.S.; Marahiel, M.; Lührmann, R. The 20kD protein of human [U4/U6.U5] tri-snRNPs is a novel cyclophilin that forms a complex with the U4/U6-specific 60kD and 90kD proteins. *RNA (New York, N.Y.)* 1998, *4*, 127-141.

31. Reidt, U.; Wahl, M.C.; Fasshauer, D.; Horowitz, D.S.; Lührmann, R.; Ficner, R. Crystal structure of a complex between human spliceosomal cyclophilin H and a U4/U6 snRNP-60K peptide. *Journal of Molecular Biology* 2003, *331*, 45-56.

32. Ingelfinger, D.; Gothel, S.F.; Marahiel, M.A.; Reidt, U.; Ficner, R.; Luhrmann, R.; Achsel, T. Two protein-protein interaction sites on the spliceosome-associated human cyclophilin CypH. *Nucleic Acids Res* 2003, *31*, 4791-4796.

33. Vidovic, I.; Nottrott, S.; Hartmuth, K.; Lührmann, R.; Ficner, R. Crystal structure of the spliceosomal 15.5 kD protein bound to a U4 snRNA fragment. *Molecular cell* 2000, *6*, 1331-1342.

34. Cvitkovic, I.; Jurica, M.S. Spliceosome database: a tool for tracking components of the spliceosome. *Nucleic Acids Res* 2013, *41*, D132-141, doi:10.1093/nar/gks999.

35. Agafonov, D.E.; Deckert, J.; Wolf, E.; Odenwalder, P.; Bessonov, S.; Will, C.L.; Urlaub, H.; Luhrmann, R. Semiquantitative Proteomic Analysis of the Human Spliceosome via a Novel Two-Dimensional Gel Electrophoresis Method. *Molecular and Cellular Biology* 2011, *31*, 2667-2682.

36. Structural Genomics Consortium. Available online: www.thesgc.org/ (accessed on 10/30/2018)

37. Wang, Y.; Han, R.; Zhang, W.; Yuan, Y.; Zhang, X.; Long, Y.; Mi, H. Human CyP33 binds specifically to mRNA and binding stimulates PPIase activity of hCyP33. *FEBS Letters* 2008, *582*, 835-839.

38. Joint Center for Structural Genomics. Available online: http://www.jcsg.org/ (accessed on 10/30/2018)

39. RIKEN. Available online: http://www.riken.jp/en/ (accessed on 10/30/2018)

40. Wang, Z.; Song, J.; Milne, T.A.; Wang, G.G.; Li, H.; Allis, C.D.; Patel, D.J. Pro Isomerization in MLL1 PHD3-Bromo Cassette Connects H3K4me Readout to CyP33 and HDAC-Mediated Repression. *Cell* 2010, *141*, 1183-1194.

41. Park, S.; Osmers, U.; Raman, G.; Schwantes, R.H.; Diaz, M.O.; Bushweller, J.H. The PHD3 Domain of MLL Acts as a CYP33-Regulated Switch between MLL-Mediated Activation and Repression. *Biochemistry* 2010, *49*, 6576-6586.

42. Hom, R.A.; Chang, P.Y.; Roy, S.; Musselman, C.A.; Glass, K.C.; Selezneva, A.I.; Gozani, O.; Ismagilov, R.F.; Cleary, M.L.; Kutateladze, T.G. Molecular mechanism of MLL PHD3 and RNA recognition by the Cyp33 RRM domain. *Journal of molecular biology* 2010, *400*, 145-154.

43. Kuraoka, I.; Ito, S.; Wada, T.; Hayashida, M.; Lee, L.; Saijo, M.; Nakatsu, Y.; Matsumoto, M.; Matsunaga, T.; Handa, H., et al. Isolation of XAB2 Complex Involved in Pre-mRNA Splicing, Transcription, and Transcription-coupled Repair. *Journal of Biological Chemistry* 2007, *283*, 940-950.

44. De, I.; Bessonov, S.; Hofele, R.; dos Santos, K.; Will, C.L.; Urlaub, H.; Luhrmann, R.; Pena, V. The RNA helicase Aquarius exhibits structural adaptations mediating its recruitment to spliceosomes. *Nat Struct Mol Biol* 2015, *22*, 138-144, doi:10.1038/nsmb.2951.

45. Huang, L.L.; Zhao, X.M.; Huang, C.Q.; Yu, L.; Xia, Z.X. Structure of recombinant human cyclophilin J, a novel member of the cyclophilin family. *Acta Crystallogr D Biol Crystallogr* 2005, *61*, 316-321, doi:10.1107/S0907444904033189.

46. Hatakeyama, S.; Nakayama, K.I. U-box proteins as a new family of ubiquitin ligases. *Biochem Biophys Res Commun* 2003, *302*, 635-645.

47. Korneta, I.; Magnus, M.; Bujnicki, J.M. Structural bioinformatics of the human spliceosomal proteome. *Nucleic Acids Res* 2012, *40*, 7046-7065, doi:10.1093/nar/gks347.

48. Mishra, S.K.; Ammon, T.; Popowicz, G.M.; Krajewski, M.; Nagel, R.J.; Ares, M.; Holak, T.A.; Jentsch, S. Role of the ubiquitin-like protein Hub1 in splice-site usage and alternative splicing. *Nature* 2011, *474*, 173-178.

49. Schimmel, J.; Balog, C.I.; Deelder, A.M.; Drijfhout, J.W.; Hensbergen, P.J.; Vertegaal, A.C. Positively charged amino acids flanking a sumoylation consensus tetramer on the 110kDa tri-snRNP component SART1 enhance sumoylation efficiency. *J Proteomics* 2010, *73*, 1523-1534, doi:10.1016/j.jprot.2010.03.008.

50. Vander Kooi, C.W.; Ohi, M.D.; Rosenberg, J.A.; Oldham, M.L.; Newcomer, M.E.; Gould, K.L.; Chazin, W.J. The Prp19 U-box Crystal Structure Suggests a Common Dimeric Architecture for a Class of Oligomeric E3 Ubiquitin Ligases † , ‡. *Biochemistry* 2006, *45*, 121-130.

831 51. Ohi, M.D.; Vander Kooi, C.W.; Rosenberg, J.A.; Chazin, W.J.; Gould, K.L. Structural insights
832 into the U-box, a domain associated with multi-ubiquitination. *Nat Struct Biol* 2003, *10*, 250-255,
833 doi:10.1038/nsb906.

834 52. Makarova, O.V.; Makarov, E.M.; Luhrmann, R. The 65 and 110 kDa SR-related proteins of
835 the U4/U6.U5 tri-snRNP are essential for the assembly of mature spliceosomes. *EMBO J* 2001, *20*,
836 2553-2563, doi:10.1093/emboj/20.10.2553.

837 53. UniprotKB. Available online: www.uniprot.org (accessed on 10/30/2018)

838 54. Chen, J.; Liefke, R.; Jiang, L.; Wang, J.; Huang, C.; Gong, Z.; Schiene-Fischer, C.; Yu, L.
839 Biochemical Features of Recombinant Human Cyclophilin J. *Anticancer Res* 2016, *36*, 1175-1180.

840 55. Ulrich, A.; Wahl, M.C. Structure and evolution of the spliceosomal peptidyl-prolyl cis-trans
841 isomerase Cwc27. *Acta Crystallogr D Biol Crystallogr* 2014, *70*, 3110-3123,
842 doi:10.1107/S1399004714021695.

843 56. Stegmann, C.M.; Seeliger, D.; Sheldrick, G.M.; de Groot, B.L.; Wahl, M.C. The
844 thermodynamic influence of trapped water molecules on a protein-ligand interaction. *Angew*
845 *Chem Int Ed Engl* 2009, *48*, 5207-5210, doi:10.1002/anie.200900481.

846 57. Nguyen, T.H.; Galej, W.P.; Bai, X.C.; Oubridge, C.; Newman, A.J.; Scheres, S.H.; Nagai, K.
847 Cryo-EM structure of the yeast U4/U6.U5 tri-snRNP at 3.7 A resolution. *Nature* 2016, *530*, 298-302,
848 doi:10.1038/nature16940.

849 58. Agafonov, D.E.; Kastner, B.; Dybkov, O.; Hofele, R.V.; Liu, W.T.; Urlaub, H.; Luhrmann, R.;
850 Stark, H. Molecular architecture of the human U4/U6.U5 tri-snRNP. *Science* 2016, *351*, 1416-1420,
851 doi:10.1126/science.aad2085.

852 59. Nguyen, T.H.; Galej, W.P.; Bai, X.C.; Savva, C.G.; Newman, A.J.; Scheres, S.H.; Nagai, K. The
853 architecture of the spliceosomal U4/U6.U5 tri-snRNP. *Nature* 2015, *523*, 47-52,
854 doi:10.1038/nature14548.

855 60. Tejedor, J.R.; Papasaikas, P.; Valcarcel, J. Genome-wide identification of Fas/CD95
856 alternative splicing regulators reveals links with iron homeostasis. *Mol Cell* 2015, *57*, 23-38,
857 doi:10.1016/j.molcel.2014.10.029.

858 61. Papasaikas, P.; Tejedor, J.R.; Vigevani, L.; Valcarcel, J. Functional splicing network reveals
859 extensive regulatory potential of the core spliceosomal machinery. *Mol Cell* 2015, *57*, 7-22,
860 doi:10.1016/j.molcel.2014.10.030.

861 62. Javadov, S.; Kuznetsov, A. Mitochondrial permeability transition and cell death: the role of
862 cyclophilin d. *Front Physiol* 2013, *4*, 76, doi:10.3389/fphys.2013.00076.

863 63. Wear, M.A.; Nowicki, M.W.; Blackburn, E.A.; McNae, I.W.; Walkinshaw, M.D. Thermo-
864 kinetic analysis space expansion for cyclophilin-ligand interactions - identification of a new
865 nonpeptide inhibitor using Biacore T200. *FEBS Open Bio* 2017, *7*, 533-549, doi:10.1002/2211-
866 5463.12201.

867 64. Daum, S.; Schumann, M.; Mathea, S.; Aumüller, T.; Balsley, M.A.; Constant, S.L.; de Lacroix,
868 B.F.a.; Kruska, F.; Braun, M.; Schiene-Fischer, C. Isoform-Specific Inhibition of Cyclophilins.
869 *Biochemistry* 2009, *48*, 6268-6277.